

Preparation, structure and properties of trinuclear $[M_3Se_4(CN)_9]^{5-}$ ($M = Mo$ or W) complexes obtained from M_3Se_7 core compounds and related studies†

Vladimir P. Fedin, Gert J. Lamprecht, Takamitsu Kohzuma, William Clegg, Mark R. J. Elsegood and A. Geoffrey Sykes *

Department of Chemistry, The University of Newcastle, Newcastle upon Tyne NE1 7RU, UK

The preparations of $[Mo_3Se_4(CN)_9]^{5-}$ and $[W_3Se_4(CN)_9]^{5-}$ by reacting polymeric $\{M_3Se_7Br_4\}_x$ or the derivative $[M_3Se_7Br_6]^{2-}$ ions ($M = Mo$ or W) with CN^- are described. Both products were isolated as the $Cs_2[M_3Se_4(CN)_9] \cdot CsCl \cdot 4H_2O$ salts. The crystal structures are essentially the same with corresponding cell dimensions within 0.3% of each other, and those for the W compound slightly the larger. The M_3Se_4 cores (approximate symmetry C_{3v}) can be described as distorted incomplete cubes with, in the tungsten case, $d_{ave}(W-W)$ 2.829, $d_{ave}(W-\mu-Se)$ 2.449, $d_{ave}(W-\mu_3-Se)$ 2.497, $d_{ave}(W-C)$ 2.179 and $d_{ave}(C-N)$ 1.16 Å. A different feature as compared to the sulfide analogues is the weak dimerisation of two trimer units giving short $Se \cdots Se$ contacts (≈ 3.5 Å). The UV/VIS spectra of brown $[Mo_3Se_4(CN)_9]^{5-}$ and green $[W_3Se_4(CN)_9]^{5-}$ indicate a red shift on replacing Mo by W , and a similar shift on exchanging S for Se . In electrochemical studies using cyclic, square-wave and differential pulse voltammetric techniques reduction potentials for the $[M_3Se_4(CN)_9]^{5-6-}$ couple (vs. normal hydrogen electrode) of -0.63 (Mo) and -0.97 V (W) were obtained. Using a $Hg-Au$ electrode two additional reduction steps were observed, and there is evidence for the formation of Hg -containing heterometallic clusters. Properties of the two aqua ions $[M_3Se_7(H_2O)_6]^{4+}$ were also studied, where these are similarly converted to $[M_3Se_4(CN)_9]^{5-}$ by Se -abstraction and substitution of H_2O by CN^- .

Since their first preparation in the mid/late 1980s,¹⁻⁴ the trinuclear incomplete cuboidal clusters $[Mo_3S_4(H_2O)_9]^{4+}$ and $[W_3S_4(H_2O)_9]^{4+}$ with a vacant metal subsite have attracted much attention.⁵⁻⁹ Both M^{IV}_3 ions have high stability in acidic solutions, and are lead-in compounds for a series of heterometallic cuboidal clusters, particularly extensive in the case of Mo .⁷⁻⁹ More recently the sulfur-rich cluster $[Mo_3S_7(H_2O)_6]^{4+}$ and its selenium analogue $[Mo_3Se_7(H_2O)_6]^{4+}$ have been prepared and their solution chemistry explored.^{10,11} These clusters have for example a single $\mu_3(S)$ and three $\mu(S_2)$ bridging ligands, with each disulfido group orientated sideways and $\eta^2: \eta^2$ to the two Mo atoms it bridges. One of the S atoms is equatorial and the other axial to the Mo_3 plane.^{12,13} In this paper the aqua ion $[W_3Se_7(H_2O)_6]^{4+}$ has been prepared for the first time from polymeric $\{W_3Se_7Br_4\}_x$ and its properties are considered alongside those of $[Mo_3Se_7(H_2O)_6]^{4+}$.¹¹ With CN^- , Se abstraction is observed together with CN^- replacement of H_2O ligands yielding $[Mo_3Se_4(CN)_9]^{5-}$ and $[W_3Se_4(CN)_9]^{5-}$. The structure of the tellurium analogue $[Mo_3Te_7(CN)_6]^{2-}$ has been reported, but no Te abstraction is observed with CN^- .¹⁴ Structures of the salts of $[Mo_3Se_4(NCS)_9]^{5-}$ and $[W_3Se_4(NCS)_9]^{5-}$ have contributed to the characterisation of M_3Se_4 cores.¹⁵⁻¹⁷

Experimental

Preparation of starting materials

The polymeric chain compounds $\{Mo_3Se_7Br_4\}_x$ and $\{W_3Se_7Br_4\}_x$ were first prepared by direct combination of the elements.^{11,13} To convert to the tetraphenylphosphonium salt of discrete anions these were heated under N_2 in a melt of PPh_4Br (1.5 g of Mo or W compound) at $280^\circ C$ for 3 h. The cold melt was ground, washed free of PPh_4Br using ethanol, and the products $[PPh_4]_2[Mo_3Se_7Br_6]$ and $[PPh_4]_2[W_3Se_7Br_6]$ used without further purification.

Other reagents

The strong acid *p*-toluenesulfonic acid (Hpts, Aldrich), potassium cyanide (BDH), triphenylphosphine, PPh_3 (Aldrich, 5% solution in toluene) and the water soluble sodium tris-(3-sulfonatophenyl)phosphine tetrahydrate, $Na_3(3-SO_3C_6H_4)_3P \cdot 4H_2O$ (Strem) referred to as PR_3^{3-} were used. Samples of the latter were shown to contain 10.3% phosphine oxide impurity using ^{31}P NMR spectroscopy. All other reagents were of analytical grade purity.

X-Ray crystallography

Crystal data for $Cs_2[W_3Se_4(CN)_9] \cdot CsCl \cdot 4H_2O$: $C_9H_6ClCs_6N_9O_4Se_4W_3$, $M = 2006.5$, triclinic, space group $P\bar{1}$, $a = 11.842(10)$, $b = 12.219(9)$, $c = 14.671(12)$ Å, $\alpha = 90.50(4)$, $\beta = 112.40(4)$, $\gamma = 115.27(3)^\circ$, $U = 1737(2)$ Å³, $Z = 2$, $D_c = 3.836$ g cm⁻³, $\mu = 20.40$ mm⁻¹ ($Mo-K\alpha$, $\lambda = 0.71073$ Å), $F(000) = 1724$, $T = 160$ K. A crystal of size $0.38 \times 0.29 \times 0.29$ mm was examined on a Stoe-Siemens four-circle diffractometer. Cell parameters were refined from 2θ values ($30-40^\circ$) of 30 reflections measured at $\pm\omega$ to minimise systematic errors. Intensities were measured with ω - θ scans and on-line profile fitting.¹⁸ 6716 measured reflections ($2\theta \leq 50^\circ$), corrected semiempirically for absorption (transmission 0.077–0.109), yielded 6081 unique data ($R_{int} = 0.0730$) for structure solution (direct methods) and refinement (least-squares on F^2 values with weighting $w^{-1} = \sigma^2(F_o^2) + (0.0862P)^2 + 42.0712P$, where $P = (F_o^2 + 2F_c^2)/3$). One Cs^+ ion is disordered over two sites. Hydrogen atoms were not located, C and N atoms were refined with isotropic, other atoms with anisotropic displacement parameters. An isotropic extinction parameter x was refined to 0.00160(15), whereby $F_c = F_o/(1 + 0.001x\lambda^3 F_c^2/\sin 2\theta)^{1/2}$. Final $R' = \{\Sigma[w(F_o^2 - F_c^2)^2]/\Sigma[w(F_o^2)^2]\}^{1/2} = 0.1459$ for all data, conventional $R = 0.0514$ on F values of 5708 reflections having $F_o^2 > 2\sigma(F_o^2)$, goodness of fit = 1.116 on all F^2 values with 246 refined parameters. Some difference electron density peaks of up to $4 e \text{ \AA}^{-3}$ lay close to heavy atoms. Programs: SHELXTL¹⁹ and local

† Non-SI unit employed: $M = \text{mol dm}^{-3}$.

Table 1 Selected bond lengths (Å) and angles (°) for Cs₅[W₃Se₄(CN)₉]·CsCl·4H₂O

W(1)–W(2)	2.840(3)	W(1)–Se(1)	2.498(2)
W(1)–W(3)	2.822(2)	W(2)–Se(1)	2.494(3)
W(2)–W(3)	2.826(2)	W(3)–Se(1)	2.498(2)
W(1)–Se(2)	2.446(2)	W(1)–Se(4)	2.441(2)
W(2)–Se(2)	2.445(2)	W(2)–Se(3)	2.454(2)
W(3)–Se(3)	2.460(3)	W(3)–Se(4)	2.447(2)
W(1)–C(1)	2.157(15)	W(1)–C(2)	2.190(14)
W(1)–C(3)	2.178(13)	W(2)–C(4)	2.193(13)
W(2)–C(5)	2.153(13)	W(2)–C(6)	2.173(14)
W(3)–C(7)	2.178(14)	W(3)–C(8)	2.180(14)
W(3)–C(9)	2.201(13)	C(1)–N(1)	1.15(2)
C(2)–N(2)	1.161(19)	C(3)–N(3)	1.178(18)
C(4)–N(4)	1.162(19)	C(5)–N(5)	1.173(19)
C(6)–N(6)	1.14(2)	C(7)–N(7)	1.167(19)
C(8)–N(8)	1.16(2)	C(9)–N(9)	1.151(19)
W(3)–W(1)–W(2)	59.87(4)	W(3)–W(2)–W(1)	59.76(5)
W(1)–W(3)–W(2)	60.37(6)	Se(4)–W(1)–Se(2)	100.80(7)
Se(4)–W(1)–Se(1)	108.23(6)	Se(2)–W(1)–Se(1)	107.23(8)
Se(2)–W(2)–Se(3)	99.75(6)	Se(2)–W(2)–Se(1)	107.39(8)
Se(3)–W(2)–Se(1)	108.62(7)	Se(4)–W(3)–Se(3)	99.19(9)
Se(4)–W(3)–Se(1)	108.05(6)	Se(3)–W(3)–Se(1)	108.30(7)
W(2)–Se(1)–W(3)	68.95(6)	W(2)–Se(1)–W(1)	69.35(8)
W(3)–Se(1)–W(1)	68.80(5)	W(2)–Se(2)–W(1)	70.98(8)
W(2)–Se(3)–W(3)	70.19(6)	W(1)–Se(4)–W(3)	70.53(5)

programs. Selected bond lengths and angles are given in Table 1.

Crystal data for Cs₅[Mo₃Se₄(CN)₉]·CsCl·4H₂O: C₉H₈ClCs₆Mo₃N₉O₄Se₄, *M* = 1742.8, triclinic, space group *P*1̄, *a* = 11.818(10), *b* = 12.191(8), *c* = 14.635(8) Å, α = 90.94(5), β = 112.23(6), γ = 115.16(5)°, *U* = 1727(2), *Z* = 2, *D*_c = 3.352 g cm⁻³, μ = 11.6 mm⁻¹, *F*(000) = 1532, *T* = 160 K. Intensity data were not measured.

Atomic coordinates, thermal parameters, and bond lengths and angles have been deposited at the Cambridge Crystallographic Data Centre (CCDC). See Instructions for Authors, *J. Chem. Soc., Dalton Trans.*, 1997, Issue 1. Any request to the CCDC for this material should quote the full literature citation and the reference number 186/467.

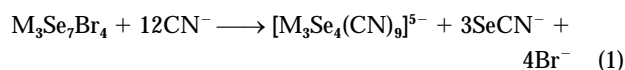
Electrochemical measurements

These were carried out using a computer-interfaced PAR Model 173 potentiostat. Prior to each experiment, the glassy carbon electrode was polished with 0.3 mm alumina, sonicated for 1 min, and rinsed thoroughly with distilled water. A mercury–gold electrode was prepared by coating a freshly polished gold electrode surface with triply-distilled mercury, and can be considered as equivalent to a hanging mercury-drop electrode. The working compartment was made air-free by passing N₂ through the electrochemical cell. The reference electrode was Ag–AgCl, and a platinum wire counter electrode was used. Potassium chloride (0.10 M) was the supporting electrolyte in all cases.

Results and Discussion

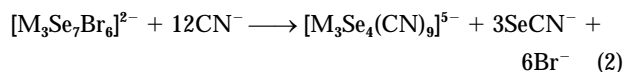
Preparation of [M₃Se₄(CN)₉]⁵⁻ clusters (M = Mo or W)

The most direct method was by treating the polymeric material {M₃Se₇Br₄}_{*x*} with CN⁻, and is the same for both M = Mo and W. A suspension of {M₃Se₇Br₄}_{*x*} (1 g) in an aqueous solution of KCN (1 g in 10 cm³) was stirred for ≈60 min [equation (1)].



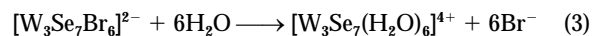
After filtering, CsCl (1 g) was added. The solutions, brown for [Mo₃Se₄(CN)₉]⁵⁻ and green for [W₃Se₄(CN)₉]⁵⁻, were kept at ambient temperatures for 5–7 d (volume 2–3 cm³). Dark brown (Mo) or green (W) crystals of Cs₅[M₃Se₄(CN)₉]·CsCl·4H₂O

separated, were filtered off and washed with diethyl ether. Yield 0.65 g (43% for Mo) and 0.54 g (38% for W). Alternatively the reactions of [PPh₄]₂[M₃Se₇Br₆] with CN⁻ [equation (2)] could be used.

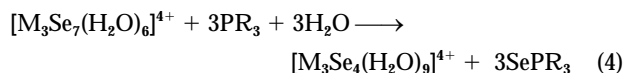


Preparation of solutions of [M₃Se₇(H₂O)₆]⁴⁺ (M = Mo or W)

The procedure in the case of [Mo₃Se₇(H₂O)₆]⁴⁺ has been described in an earlier study.¹¹ The tungsten analogue was prepared by a similar method [equation (3)]. Thus a solution of

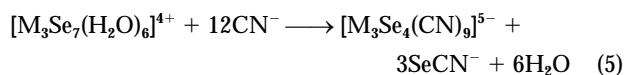


[PPh₄]₂[W₃Se₇Br₆] (0.5 g) in 4 M Hpts (50 cm³) was kept at 50–60 °C for 6 h. The yellow-orange solution obtained after filtration was diluted seven-fold with H₂O and loaded onto a Dowex 50W-X2 cation-exchange resin column. A well defined tight band at the top of the column was eluted with strong acid, e.g. 2–4 M Hpts. Inductively coupled plasma analyses gave a Mo to Se ratio of 3:7.2 for [Mo₃Se₇(H₂O)₆]⁴⁺, and 3:7.1 for [W₃Se₇(H₂O)₆]⁴⁺. Solution yields were [Mo₃Se₇(H₂O)₆]⁴⁺ (44%) and [W₃Se₇(H₂O)₆]⁴⁺ (35%). Increasing absorbance is observed towards the UV with shoulders only at ≈370 (ε = 1150) and ≈480 (200) for [Mo₃Se₇(H₂O)₆]⁴⁺, and ≈375 (1014) and ≈500 nm (330 M⁻¹ cm⁻¹ per M₃) for [W₃Se₇(H₂O)₆]⁴⁺. More definitive are the [M₃Se₄(H₂O)₉]⁴⁺ UV/VIS spectra obtained on reacting [M₃Se₇(H₂O)₆]⁴⁺ in 2–3 M Hpts (50 cm³) with 5% triphenylphosphine in toluene (5 cm³) (solutions were stirred for ≈20 min), or with a ≈ten-fold excess of the water-soluble phosphine PR₃³⁻, when faster conversions were observed. Peak positions are at 425 (ε = 2460) and 648 (263) for [Mo₃Se₄(H₂O)₉]⁴⁺,¹⁵ and 359 (≈6660) and 618 nm (≈547 M⁻¹ cm⁻¹) for [W₃Se₄(H₂O)₉]⁴⁺. In both phosphine reactions the μ-diselenide bonds are cleaved and Se abstraction occurs, equation (4).



Conversion of [M₃Se₇(H₂O)₆]⁴⁺ into [M₃Se₄(CN)₉]⁵⁻ (M = Mo or W)

Solutions of [M₃Se₇(H₂O)₆]⁴⁺ in 2 M Hpts were diluted to [H⁺] = 0.5 M and loaded onto a Dowex 50W-X2 column. After washing with water elution was with 0.1 M KCN. Abstraction of Se by CN⁻, and CN⁻ replacement of H₂O occurs, equation (5).



Conversion of [M₃Se₄(H₂O)₉]⁴⁺ into [M₃Se₄(CN)₉]⁵⁻ (M = Mo or W)

A solution of [M₃Se₄(H₂O)₉]⁴⁺ in 2 M HCl was taken to dryness on a vacuum line and a solution of 0.1 M KCN added. Alternatively [M₃Se₄(H₂O)₉]⁴⁺ was eluted from a cation-exchange column with 0.1 M CN⁻. Substitution of H₂O by CN⁻ gives [M₃Se₄(CN)₉]⁵⁻. In none of these reactions are M–Se–M bridges cleaved by the concentrations of CN⁻ used. A similar situation applies for the sulfido-bridged cluster [Mo₃S₄(H₂O)₉]⁴⁺.²⁰

Structures

The structure of the [W₃Se₄(CN)₉]⁵⁻ anion is shown in Fig. 1. It has essentially C_{3v} symmetry with one μ₃-Se and three μ₂-Se. Mean bond lengths are W–W 2.829, W–μ₂-Se 2.449, W–μ₃-Se 2.497, W–C 2.179 and C–N 1.16 Å. Crystals of the corresponding

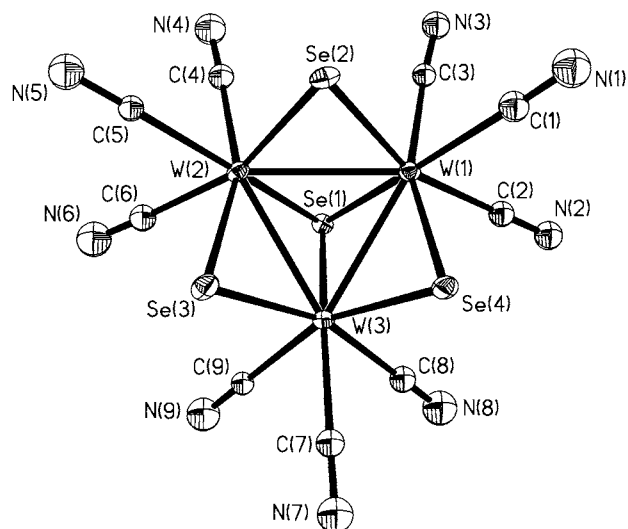


Fig. 1 Structure of the $[\text{W}_3\text{Se}_4(\text{CN})_9]^{5-}$ anion showing the atom labeling scheme and 50% probability displacement ellipsoids

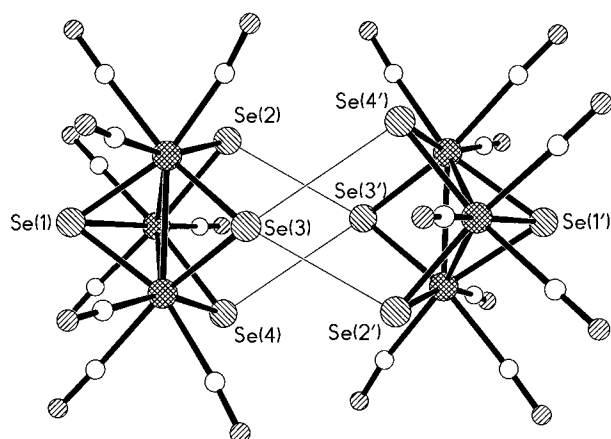


Fig. 2 Structure of the $[\text{W}_3\text{Se}_4(\text{CN})_9]^{5-}$ anions showing Se...Se interactions between two adjacent clusters

molybdenum complex are isomorphous, with cell axes differing by less than 0.3%, so the structure is probably insignificantly different. The W–Se bonds are slightly longer than those in the $[\text{W}_3\text{Se}_4(\text{NCS})_9]^{5-}$ anion (mean $\text{W}-\mu_2\text{-Se}$ 2.393, $\text{W}-\mu_3\text{-Se}$ 2.458 Å),¹⁷ and the Mo–Se bonds in $[\text{Mo}_3\text{Se}_4(\text{NCS})_9]^{5-}$ (mean $\text{Mo}-\mu_2\text{-Se}$ 2.409, $\text{Mo}-\mu_3\text{-Se}$ 2.452 Å).¹⁵ These are the only previously reported structures with incomplete cuboidal M_3Se_4 cores (M = Mo or W). The same type of structure is well known for the M_3S_4 core; the most recent release of the Cambridge Structural Database²¹ contains 16 structures of W complexes and 31 structures of Mo complexes. The overall geometry of these M_3S_4 cores is essentially the same as for the M_3Se_4 cores, except that the smaller sulfur atoms lead to shorter M–S bonds, ranging from 2.237 to 2.353 Å for $\text{W}-\mu_2\text{-S}_2$, from 2.331 to 2.404 Å for $\text{W}-\mu_3\text{-S}$, from 2.238 to 2.393 Å for $\text{Mo}-\mu_2\text{-S}$, and from 2.317 to 2.421 Å for $\text{Mo}-\mu_3\text{-S}$.

As found previously for the $[\text{W}_3\text{Se}_4(\text{NCS})_9]^{5-}$ anion,¹⁷ the $[\text{W}_3\text{Se}_4(\text{CN})_9]^{5-}$ anion in the present structure is weakly dimerised through Se...Se interactions, Fig. 2. The observed distances are 3.415 for $\text{Se}(2)\cdots\text{Se}(3')$ and 3.686 Å for $\text{Se}(4)\cdots\text{Se}(3')$, comparable to the distances of 3.361–3.585 Å in the $[\text{W}_3\text{Se}_4(\text{NCS})_9]^{5-}$ weak dimer,¹⁷ and shorter than the intramolecular distances of 3.737–3.746 Å between pairs of μ_2 -Se atoms in the present structure.

UV/VIS spectra

Peak positions λ/nm ($\epsilon/\text{M}^{-1}\text{cm}^{-1}$ per trimer) were obtained for both $[\text{M}_3\text{Se}_4(\text{CN})_9]^{5-}$ clusters (Fig. 3) and are 350 (5070), 443 (5460), 677 (730) (M = Mo); and 322 (8700), 387 (6200), 622 (860) (M = W). The spectrum of $[\text{Mo}_3\text{S}_4(\text{CN})_9]^{5-}$, 342 (4500),

Table 2 A comparison of the lowest energy transition in the UV/VIS electronic spectra λ/nm ($\epsilon/\text{M}^{-1}\text{cm}^{-1}$ per M_3) for M_3Y_4 clusters (M = Mo or W, Y = S or Se)

Cluster	Mo/S	W/S	Mo/Se	W/Se
$[\text{M}_3\text{Y}_4(\text{H}_2\text{O})_9]^{4+}$ in 2 M Hpts	602 (251) ^a	560 (490) ^a	648 (263) ^b	618
$[\text{M}_3\text{Y}_4(\text{H}_2\text{O})_9]^{4+}$ in 1 M HCl	620 (315) ^a	570 (480) ^a	677 ^c	623 ^d
$[\text{M}_3\text{Y}_4(\text{CN})_9]^{5-}$ in H_2O	610 (500) ^e	579 (370) ^f	677 (730)	611 (860)
$[\text{M}_3\text{Y}_4(\text{NCS})_9]^{5-}$ in 1 M NCS		640 (730) ^a		680

^a Refs. 5 and 6. ^b Ref. 15. ^c Absorbance ratio $A_{431}:A_{677} = 11.2$. ^d Absorbance ratio $A_{358}:A_{623} = 13.6$. ^e Ref. 18. ^f Ref. 24.

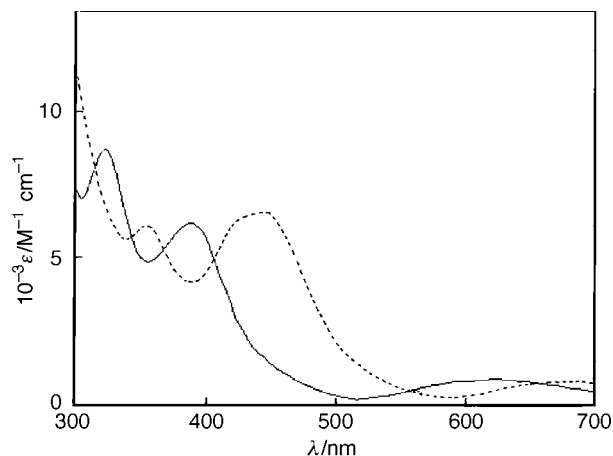


Fig. 3 The UV/VIS spectra of $[\text{Mo}_3\text{Se}_4(\text{CN})_9]^{5-}$ (---) and $[\text{W}_3\text{Se}_4(\text{CN})_9]^{5-}$ (—) in H_2O

377 (5500), 610 (500) has been reported previously.²⁰ The relative peak positions $\text{Mo} > \text{W}$ indicate higher energy ligand-to-metal charge transfer (LMCT) transitions for the W cluster, and $\text{Se} > \text{S}$ with the higher energy transitions for the S clusters. Both effects correlate with known redox properties of the elements. Thus in the $[\text{IrCl}_6]^{2-}$ oxidations of $[\text{M}^{\text{V}}_2\text{O}_4(\text{H}_2\text{O})_6]^{2+}$ and $[\text{M}^{\text{IV}}_3\text{O}_4(\text{H}_2\text{O})_9]^{4+}$ the M = W reactions are 10^5 – 10^6 times faster than those with M = Mo.²² Also the electronegativity of sulfur is greater than that of selenium. Müller *et al.*²⁰ have reported molecular orbital calculations relating to the electronic structures of $[\text{Mo}_3\text{S}_4(\text{CN})_9]^{5-}$ and other Mo–S complexes. These show that the bonding within a central Mo_xS_y moiety is rather localised (70–80% Mo 4d and S 3p). Li *et al.*²³ on the other hand have reported calculations consistent with delocalisation and multiple bonding in the quasi-aromatic $\text{Mo}_3(\mu_2\text{-S})_3$ fragment of the $\text{Mo}_3\text{S}_4^{4+}$ core. An additional band for $[\text{Mo}_3\text{Se}_4(\text{CN})_9]^{5-}$ at 247 nm ($\epsilon = 17\,000\text{ M}^{-1}\text{cm}^{-1}$ per Mo_3) is observed also for $[\text{Mo}_3\text{S}_4(\text{CN})_9]^{5-}$, and is assigned to $\text{CN}\rightarrow\text{Mo}$ charge transfer. Data for the lower energy peaks in the visible region for $[\text{M}_3\text{Y}_4(\text{H}_2\text{O})_9]^{4+}$ (M = Mo or W; Y = S or Se) in 2 M Hpts and 1 M HCl, and for $[\text{M}_3\text{Y}_4(\text{CN})_9]^{5-}$ and $[\text{M}_3\text{Y}_4(\text{NCS})_9]^{5-}$ (N bonded) are given in Table 2. Trends observed for the thiocyanato complexes are an interesting feature indicating a greater ‘mixing in’ with this terminal ligand.

Electrochemical studies

The Mo^{IV}_3 cluster $[\text{Mo}_3\text{Se}_4(\text{CN})_9]^{5-}$ gives an irreversible cyclic voltammogram, Fig. 4, but a quasi-reversible response at -0.86 (average) vs. Ag–AgCl electrode (-0.63 vs. NHE), Table 3, by SWV corresponding to the $\text{Mo}^{\text{IV}}_3 + \text{e}^- \rightleftharpoons \text{Mo}^{\text{III}}\text{Mo}^{\text{IV}}_2$ change, Fig. 5. Cyclopentadienyl analogues $[\text{Mo}_3\text{S}_4\text{Cp}_3]^+$ and $[\text{Mo}_3\text{S}_4\text{Cp}_3]$ ($\text{Cp} = \eta^5\text{-C}_5\text{H}_5$) having the same core oxidation states have been studied previously.^{25,26} In the case of $[\text{Mo}_3\text{S}_4(\text{CN})_9]^{5-}$, the reduction potential for the same one-

Table 3 Summary of electrochemical data (25 °C) for $[\text{Mo}_3\text{Se}_4(\text{CN})_9]^{5-}$ and $[\text{W}_3\text{Se}_4(\text{CN})_9]^{5-}$ in aqueous solution, N_2 atmosphere, $I = 0.10 \text{ M}$ (KCl) *

Complex	Method	E_{p_c}/V	E_{p_a}/V	E_2/V	$E^{0'}/\text{V}$	Reversibility	Electrode
$[\text{Mo}_3\text{Se}_4(\text{CN})_9]^{5-}$	CV	-0.96	-0.62			irrev	GC
	SWV				-0.87		
	DPV				-0.86		
	CV	-0.86	-0.79	-0.83		q-rev	Hg-Au
	CV	-1.17	-1.11	-1.14		q-rev	
	CV	-1.39				irrev	
	SWV				-0.82		
	SWV				-1.13		
	SWV				-1.29		
	DPV				-0.83		
	DPV				-1.13		
	DPV				-1.28		
$[\text{W}_3\text{Se}_4(\text{CN})_9]^{5-}$	CV	-1.28	-1.08	-1.18		q-rev	GC
	SWV				-1.20		
	CV	-1.19	-1.09	-1.14		q-rev	Hg-Au
	CV	-1.33				irrev	
	CV	-1.67				irrev	
	SWV				-1.15		
	SWV				-1.30		
	SWV				-1.62		

* Abbreviations used: CV = cyclic voltammetry, SWV = square wave voltammetry, DPV = differential pulse voltammetry, GC = glassy carbon electrode, Hg-Au is Hg coated Au electrode, CV peak to peak separation (ΔE_p) gives E_2 if quasi-reversible (q-rev); potentials are given vs. Ag-AgCl electrode, add 0.22 V to convert to values vs. NHE.

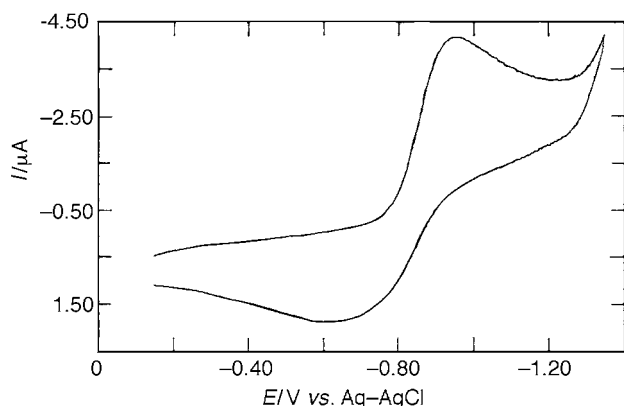


Fig. 4 Cyclic voltammogram for $[\text{Mo}_3\text{Se}_4(\text{CN})_9]^{5-}$ at a glassy carbon electrode in 0.10 M KCl, cathodic potential -0.96 V and anodic potential -0.62 V vs. Ag-AgCl electrode, irreversible behaviour indicated

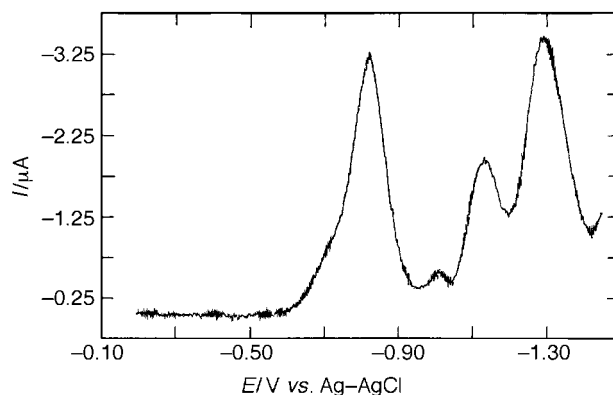


Fig. 6 Square-wave voltammogram for $[\text{Mo}_3\text{Se}_4(\text{CN})_9]^{5-}$ at a Hg-Au electrode in 0.10 M KCl, giving an $E^{0'}$ value of -0.82 V vs. Ag-AgCl (-0.60 V vs. NHE) for the $[\text{Mo}_3\text{Se}_4(\text{CN})_9]^{5-6-}$ couple and two additional peaks at -1.13 and -1.29 assigned to a Hg-adduct (see text)

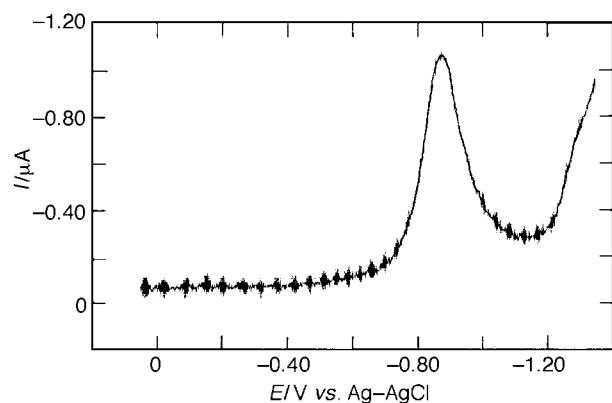


Fig. 5 Square-wave voltammogram for the $[\text{Mo}_3\text{Se}_4(\text{CN})_9]^{5-6-}$ couple giving a reduction potential $E^{0'} = -0.87 \text{ V}$ vs. Ag-AgCl (-0.65 V vs. NHE) in 0.10 M KCl

electron process has been reported as -1.49 V vs. NHE.^{20,27} It is concluded that the Se core ligands stabilize the lower 6- oxidation state. In the case of the tungsten analogue $[\text{W}_3\text{Se}_4(\text{CN})_9]^{5-}$ the reduction potential of -1.19 V vs. Ag-AgCl (-0.97 V vs. NHE), Table 3, confirms that the W^{IV} cluster is more difficult

to reduce than the Mo^{IV} . Using a glassy carbon electrode both clusters give only one redox stage for the potential range explored. Reduction potentials (vs. NHE) for the same redox change $\text{M}^{\text{IV}}_3 + e^- \rightleftharpoons \text{M}^{\text{III}}\text{M}^{\text{IV}}_2$ and other couples are for $[\text{Mo}_3\text{S}_4(\text{Hnta})_3]^{2-3-}$ (-0.42), $[\text{W}_3\text{S}_4(\text{Hnta})_3]^{2-3-}$ (-0.90), $[\text{Mo}_3\text{S}_4\text{Cl}_3(\text{dmpe})_3]^{+0}$ (-0.42) and $[\text{W}_3\text{S}_4(\text{Hnta})_3]^{2-3-}$ (-0.89 V),^{28,29} where Hnta is singly-protonated nitrilotriacetate (aqueous solutions), and dmpe = 1,2-bis(dimethylphosphino)ethane (organic solvent). Again the Mo clusters are more readily reduced. The differences observed for the Mo and W analogues of 0.48 and 0.47 V are similar to the 0.34 V value observed in the present studies.

Using a Hg-Au electrode additional redox steps are observed, e.g. Fig. 6. The first peak remains initially unchanged and is assigned to the $[\text{Mo}_3\text{Se}_4(\text{CN})_9]^{5-6-}$ couple. The two additional peaks are assigned to Hg heterometallic adducts $[\text{Mo}_3\text{HgSe}_4(\text{CN})_9]^{5-}$ or a related cluster, in which case couples such as $[\text{Mo}_3\text{HgSe}_4(\text{CN})_9]^{6-7-}$ and $[\text{Mo}_3\text{HgSe}_4(\text{CN})_9]^{7-8-}$ may be relevant. No colour changes were observed using the Hg-Au electrode. The tungsten complex gives similar behaviour with reduction potentials as listed in Table 3. A hanging mercury-drop electrode was used in the studies by Shibahara *et al.*²⁸ on the Hnta complexes, when three stages were also observed.

Conclusions

Studies on $[\text{Mo}_3\text{Se}_4(\text{CN})_9]^{5-}$ and $[\text{W}_3\text{Se}_4(\text{CN})_9]^{5-}$ have further established the chemistry of M_3Se_4 clusters. The structures have virtually identical geometries and short M–M distances observed are consistent with metal–metal bonding. Unlike aqua M_3Se_4 (and M_3S_4) complexes, electrochemical reduction is possible with the cyano products. Reduction potentials (vs. NHE) associated with the $\text{M}^{\text{IV}}_3 + \text{e}^- \rightleftharpoons \text{M}^{\text{III}}\text{M}^{\text{IV}}_2$ couple -0.63 (Mo) and -0.97 V (W) illustrate a more readily accessed redox chemistry, with Mo the more easily reduced. Previously the reduction potential for the $[\text{Mo}_3\text{S}_4(\text{CN})_9]^{5-/6-}$ couple has been reported as -1.49 V (vs. NHE),^{20,26} and from the differences in reduction potentials observed a value in the range -1.80 to -1.90 is estimated for the $[\text{W}_3\text{S}_4(\text{CN})_9]^{5-/6-}$ couple. Red shifts in the UV/VIS spectra are observed on replacing Mo with W and Se with S, consistent with LMCT transitions.

Acknowledgements

We are grateful to the Royal Society for a Kapitza Fellowship (V. P. F.), the EPSRC for Research Grants and the Universities of Bloemfontein (G. J. L.) and Ibaraki (T. K.) for study leave.

References

- 1 T. Shibahara, *Adv. Inorg. Chem.*, 1991, **37**, 143–173.
- 2 F. A. Cotton, Z. Dori, R. Llusar and W. Schwotzer, *J. Am. Chem. Soc.*, 1985, **107**, 6734.
- 3 M. Martinez, B.-L. Ooi and A. G. Sykes, *J. Am. Chem. Soc.*, 1987, **109**, 4615.
- 4 T. Shibahara, A. Takeuchi, A. Ohtsuji, K. Kohda and H. Kuroya, *Inorg. Chim. Acta*, 1987, **127**, 145.
- 5 B.-L. Ooi and A. G. Sykes, *Inorg. Chem.*, 1989, **28**, 3799.
- 6 M. Nasreldin, A. Olatunji, P. W. Dimmock and A. G. Sykes, *J. Chem. Soc., Dalton Trans.*, 1990, 1765.
- 7 D. M. Saysell, M. N. Sokolov and A. G. Sykes, *ACS Symp. Ser.*, 1996, **653**, 216–224.
- 8 M. Nasreldin, C. A. Routledge and A. G. Sykes, *J. Chem. Soc., Dalton Trans.*, 1994, 2809.
- 9 V. P. Fedin, M. N. Sokolov and A. G. Sykes, *J. Chem. Soc., Dalton Trans.*, 1996, 4089.
- 10 V. P. Fedin, G. J. Lamprecht and A. G. Sykes, *J. Chem. Soc., Chem. Commun.*, 1994, 2685.
- 11 D. M. Saysell, V. P. Fedin, M. N. Sokolov, G. J. Lamprecht and A. G. Sykes, *Inorg. Chem.*, in the press.
- 12 M. D. Meienberger, K. Hegetschweiler, H. Rielgger and V. Granlich, *Inorg. Chim. Acta*, 1993, **213**, 157.
- 13 V. P. Fedin, M. N. Sokolov, O. A. Geras'ko, A. V. Virovets, N. V. Podberezskaya and V. Y. Fedorov, *Inorg. Chim. Acta*, 1991, **187**, 81.
- 14 V. P. Fedin, H. Imoto, T. Saito, W. McFarlane and A. G. Sykes, *Inorg. Chem.*, 1995, **34**, 5097.
- 15 M. Nasreldin, G. Henkel, G. Kampmann, B. Krebs, G. J. Lamprecht, C. A. Routledge and A. G. Sykes, *J. Chem. Soc., Dalton Trans.*, 1993, 737.
- 16 G. J. Lamprecht, M. Martinez, M. Nasreldin, C. A. Routledge, N. Al-Shatti and A. G. Sykes, *J. Chem. Soc., Dalton Trans.*, 1993, 747.
- 17 V. P. Fedin, M. N. Sokolov, A. V. Virovets, N. V. Podberezskaya and V. Y. Federov, *Polyhedron*, 1992, **11**, 2973.
- 18 W. Clegg, *Acta Crystallogr., Sect. A*, 1981, **37**, 22.
- 19 G. M. Sheldrick, SHELXTL manual, revision 5, Siemens Analytical X-Ray Instruments, Madison, WI, 1994.
- 20 A. Müller, R. Jostes, W. Eltzner, C.-S. Nie, E. Diemann, H. Bögge, M. Zimmermann, M. Dartmann, U. Reinsch-Vogell, S. Che, S. J. Cyvin and B. N. Cyvin, *Inorg. Chem.*, 1985, **24**, 2872.
- 21 F. H. Allen and O. Kennard, *Chem. Des. Autom. News*, 1993, **8**, 31.
- 22 B.-L. Ooi, A. L. Petrou and A. G. Sykes, *Inorg. Chem.*, 1988, **27**, 3626.
- 23 J. Li, C.-W. Liu and J.-X. Lu, *J. Chem. Soc., Faraday Trans.*, 1994, **90**, 39.
- 24 V. P. Fedin and A. G. Sykes, unpublished work.
- 25 P. J. Vergamini, H. Vahrenkamp and L. F. Dahl, *J. Am. Chem. Soc.*, 1971, **93**, 6327.
- 26 W. Beck, W. Danzer and G. Thiel, *Angew. Chem., Int. Ed. Engl.*, 1973, **12**, 582.
- 27 K. Wieghardt, W. Herrmann, A. Müller, W. Eltzner and M. Zimmermann, *Z. Naturforsch., Teil B*, 1984, **39**, 876.
- 28 T. Shibahara, M. Yamasaki, G. Sakane, K. Minami, T. Yabuki and A. Ichimura, *Inorg. Chem.*, 1992, **31**, 640.
- 29 F. A. Cotton, R. Llusar and C. T. Eagle, *J. Am. Chem. Soc.*, 1989, **111**, 4332.

Received 21st November 1996; Paper 6/07930J